GEOLOGY | THE GEOLOGICAL SOCIETY OF AMERICA®

https://doi.org/10.1130/G52424.1

Manuscript received 29 May 2024
Revised manuscript received 26 September 2024
Manuscript accepted 9 October 2024

Published online 21 October 2024

New insights on gravity flow dynamics during submarine canyon flushing events

Marta Ribó[1,*], Joshu J. Mountjoy[2], Neil Mitchell[3], Sally J. Watson[2,4], Jasper J.L. Hoffmann[2,5,6], and Susi Woelz[2]
[1]School of Science, Auckland University of Technology, Auckland 1010, New Zealand
[2]National Institute of Water and Atmospheric Research, Wellington 6021, New Zealand
[3]Earth and Environmental Science, The University of Manchester, M13 9PL Manchester, UK
[4]Institute of Marine Sciences, University of Auckland, Auckland 1010, New Zealand
[5]Alfred-Wegener-Institute, Helmholtz Centre for Polar and Marine Research, Hafenstraße 4325992 List, Germany
[6]Marine Geology & Seafloor Surveying Group, University of Malta, Msida MSD 2080, Malta

ABSTRACT

Millions of tons of material are flushed through submarine canyons during infrequent high-magnitude events, transporting coastal sediment to the deep ocean. However, observations related to individual canyon flushing events are challenging due to the destructive nature and infrequency of flushing events. The impacts of one of the largest gravity flows in the past decade were documented in Kaikōura Canyon, Aotearoa–New Zealand, where >1 km^3 of sediment was mobilized by the 2016 CE Kaikōura earthquake (M_w 7.8). We present new high-resolution (<1 m) multibeam data collected with an autonomous underwater vehicle (AUV) along the Kaikōura Canyon axis, together with side-scan sonar and seafloor video imagery. These data sets reveal a wide range of erosional and depositional features that were not previously identified. Eroded bedrock and deep erosional structures are found in the upper canyon, including linear grooves, and rockfall debris (>5-m-diameter boulders). This erosional area transitions downcanyon to coarse-grained depositional bedforms, including cyclic steps and gravel waves (average wavelengths of 250 m and wave heights of ~20 m), covering the mid- and lower canyon. Our observations provide high-resolution field-based evidence of (1) flow transformation, from a debris flow to a high-density turbidity current; and (2) variations of flow dynamics within turbidity currents both across- and downcanyon, during an infrequent, high-energy canyon flushing event. This research offers new insights into the processes that create and shape nearshore bedrock-incising submarine canyons.

INTRODUCTION

The efficiency of submarine canyons connecting land and deep ocean is influenced by the magnitude of canyon incision into the continental shelf (Bernhardt and Schwanghart, 2021; Covault and Graham, 2010; Smith et al., 2018). However, the mechanisms by which submarine canyons are initially formed are still poorly understood. Some may form by large submarine landslides (Normark and Carlson, 2003), and some may be dominated by incision and downslope elongation (Micallef et al., 2014). Canyons can grow in relief, to some extent, simply because of hemipelagic deposition in interfluves, while channel thalwegs are starved of sediment (Mitchell, 2005). Alternatively, as we suggest for Kaikōura Canyon (off the northeast coast of South Island, Aotearoa–New Zealand), some canyons are primarily created by very large infrequent sediment flows known as submarine canyon flushing events (Talling, 2014).

During these events, large-scale sediment gravity flows, such as debris flows and turbidity currents, can transport millions of tons of material to the deep ocean, and are capable of traveling hundreds of kilometers across the seafloor (Amy and Talling, 2006; Talling et al., 2015). Coarse-grained high-concentration debris flows can support boulder-sized grains and gravel within a matrix of interstitial fluid and fine-grained sediment of finite yield strength (Middleton and Hampton, 1973). Turbidity currents develop internal stratification due to vertical gravity segregation of particles, resulting in a coarse-grained, dense basal layer near the flow front, and a less dense and turbulent upper layer of fine sediment (Stow and Smillie, 2020).

Debris flows can transform into turbidity currents, with no change in water content, when the velocity is great enough to produce internal turbulence (Fisher, 1983; Kuenen and Hough, 1951; Wang et al., 2024). The transformation from debris flow into turbidity current can result in a bipartite (two-phase) gravity flow containing a lower homogeneous flow with plastic rheology and a upper turbidity current, with Newtonian rheology (Haughton et al., 2003, 2009; Talling et al., 2004). However, most of the present understanding of gravity flow transformations is derived from theoretical descriptions, stratigraphic records, and laboratory experiments (Amy and Talling, 2006; Felix and Peakall, 2006; Felix et al., 2009; Fisher, 1983; Wang et al., 2024).

One of the largest documented gravity flows in the past decade was triggered by the 2016 CE Kaikōura M_w 7.8 earthquake, causing the canyon flushing event in the Kaikōura Canyon (Mountjoy et al., 2018). The Kaikōura Canyon comes to within 1 km of the shore south of the Kaikōura Peninsula (Fig. 1) and is one of 183 active canyons worldwide lying within 6 km of shorelines (Bernhardt and Schwanghart, 2021; Harris and Whiteway, 2011). Coarse sediment entering this canyon is derived from longshore drift, coastal erosion, and reworking of shelf deposits (Gibbs et al., 2020; Lewis and Barnes, 1999; Nokes et al., 2021).

Although the long-runout turbidity current that followed the 2016 earthquake was dominated by silt to sand (Howarth et al., 2021; Mountjoy et al., 2018), our new field-based observations within the canyon reveal the pres-

Marta Ribó https://orcid.org/0000-0002-6211-7007
*marta.ribo.gene@aut.ac.nz

CITATION: Ribó, M., et al., 2025, New insights on gravity flow dynamics during submarine canyon flushing events: Geology, v. 53, p. 34–39, https://doi.org/10.1130/G52424.1

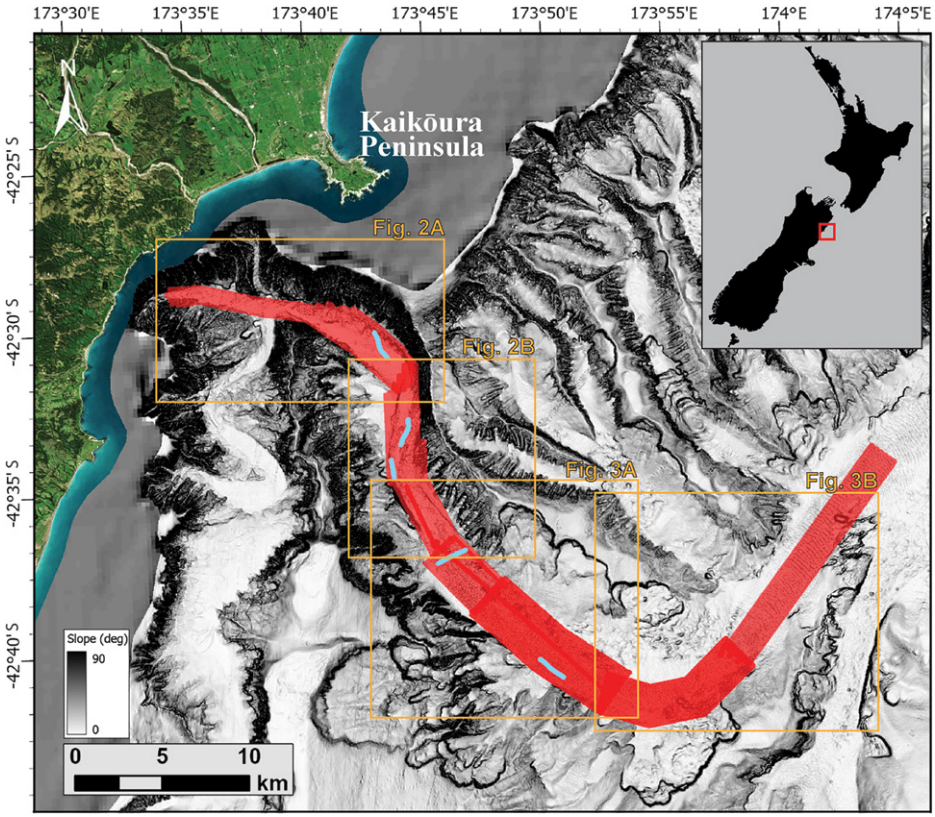

Figure 1. Slope gradient map of Kaikōura Canyon (Aotearoa–New Zealand) and surroundings (25-m grid; 250-m grid at the continental shelf), showing autonomous underwater vehicle (AUV) high-resolution multibeam data coverage (red polygons) and deep-towed imaging system (DTIS) tracks (light-blue lines) where seafloor imagery was collected. Our data, the high-resolution AUV bathymetry data, was collected during voyage TAN2011. The 25-m resolution grid, collected in 2016 during the voyage TAN1613, can be obtained upon request to NIWA. The 250-m grid is obtained from the NIWA New Zealand 250-m resolution gridded bathymetric data set (Mitchell et al., 2012)

ence of coarse sediments—including boulders up to several meters in diameter. Based on these new measurements we hypothesize that during the flushing event, a two-part sediment flow was generated: (1) a high-density debris flow of coarse sediment within the steeper upper canyon reaches, and (2) the transformation of that debris flow into a lower-density flow (turbidity current) capable of traveling long distances. Our unique geomorphic observations allow detailed interpretation of the dynamics of gravity flow transformations that occur during canyon flushing events, demonstrating how infrequent large sediment flows are a creative force for bedrock-floored submarine canyons.

DATA AND METHODS

High-resolution (<1 m) multibeam bathymetry and side-scan sonar data were acquired within the Kaikōura Canyon in October 2020 during the TAN2011 voyage onboard RV *Tangaroa* (https://niwa.co.nz/vessels/voyages/2020-kaikoura-canyons). The data were collected using the HUGIN 3000 autonomous underwater vehicle (AUV), equipped with an EdgeTech 2205 side-scan sonar system, and a Kongsberg EM2040 multibeam echosounder system (operating at bandwidths of 200–400 kHz with a coverage of 5.5 times water depth). The EdgeTech operated at 75 kHz for long-range target detection (at lower resolution) and at 410 kHz for increased resolution (though with decreased range). AUV data provided 1-m-resolution seafloor digital elevation models, used to interpret canyon geomorphology and to compute the morphological parameters (e.g., wavelength, wave height) of the depositional bedforms following the methodology described by Ribó et al. (2016). The side-scan sonar data was used to measure the dimensions of the boulders below the resolution of the multibeam data. A deep-towed imaging system (DTIS) provided high-definition imagery of the seafloor substrate. The DTIS was equipped with cameras for vertically orientated still images (24MP Nikon DSLR) and obliquely orientated video (Sony HD1018p, angled forward at 40° from vertical). Lighting was provided by LED floodlights (video) and electronic strobe (stills). Image scaling was provided by pairs of parallel red lasers aligned with each camera.

RESULTS

Seafloor imagery revealed rock blocks with sharp edges in the upper canyon (~1245 m and ~1400 m water depth). Linear grooves (30–130 m length, ~3 m average width, >10 m relief) and erosion scours (Fig. 2) were observed where maximum erosion (>50 m) occurred during the 2016 canyon flushing event (Fig. S1 in the Supplemental Material[1]).

Gravel waves develop at mid-canyon (~1450 m water depth), where the canyon axis abruptly doubles in width (i.e., from 1 km to 2 km across; Fig. 3A). These gravel waves are large, undulating coarse-grained bedforms, orientated roughly perpendicular to the dominant current flow direction, with wavelengths of 75 m to ~100 m and wave heights of ~6 m (Fig. S2). They coexist with cyclic steps (i.e., coherent trains of upstream-migrating steps; Cartigny et al., 2011; Kostic, 2011; Parker, 1996), with wavelengths of ~210 m and wave height of ~12 m (Figs. S2 and S3).

In the lower canyon, from ~1700 m water depth, larger gravel waves with wavelengths of ~250 m and wave heights of ~20 m, cover the entire canyon axis (Fig. 3B; Fig. S2). They are predominantly composed of gravel and boulders—some very large (~5 m diameter) as observed in side-scan sonar images on the down-canyon (lee) sides of the gravel waves (Figs. 3C and 3D, Fig. S4). Small-scale bedforms or dunes, with wavelengths of ~15–30 m and wave heights of 1.5–5 m, are superimposed on these larger gravel waves, with crests oriented from normal to oblique to the gravel wave crests (Figs. 3B–3D).

From mid- to lower canyon, the profile shape of the gravel waves changes from symmetrical to asymmetrical, with the steeper flanks (lee sides) facing downslope. The wave crests change shape in planform at mid-canyon from linear and crescentic to reverse crescentic, and back to linear in the lower canyon (Fig. 3). Gravel wave heights and wavelengths increase downcanyon, except where the canyon axis orientation abruptly changes (from northwest-southeast to northeast-southwest) between ~1730 m and ~1900 m water depth (Fig. 3; Fig. S2). There, gravel waves within the canyon axis coexist with erosional scours and erosive lineations observed on the canyon walls (i.e., longitudinal bedforms similar to striations or furrows that are rectilinear, parallel, and regularly spaced, aligned with the direction of the current flow; Figs. 3A and 3B).

[1]Supplemental Material. Supplemental figures: DTIS seafloor imagery showing the erosive and depositional features (Figs. S1 and S4) and the distribution downcanyon of the wave height and wavelength of the different depositional features (Figs. S2 and S3). Please visit https://doi.org/10.1130/GEOL.S.27214425 to access the supplemental material; contact editing@geosociety.org with any questions.

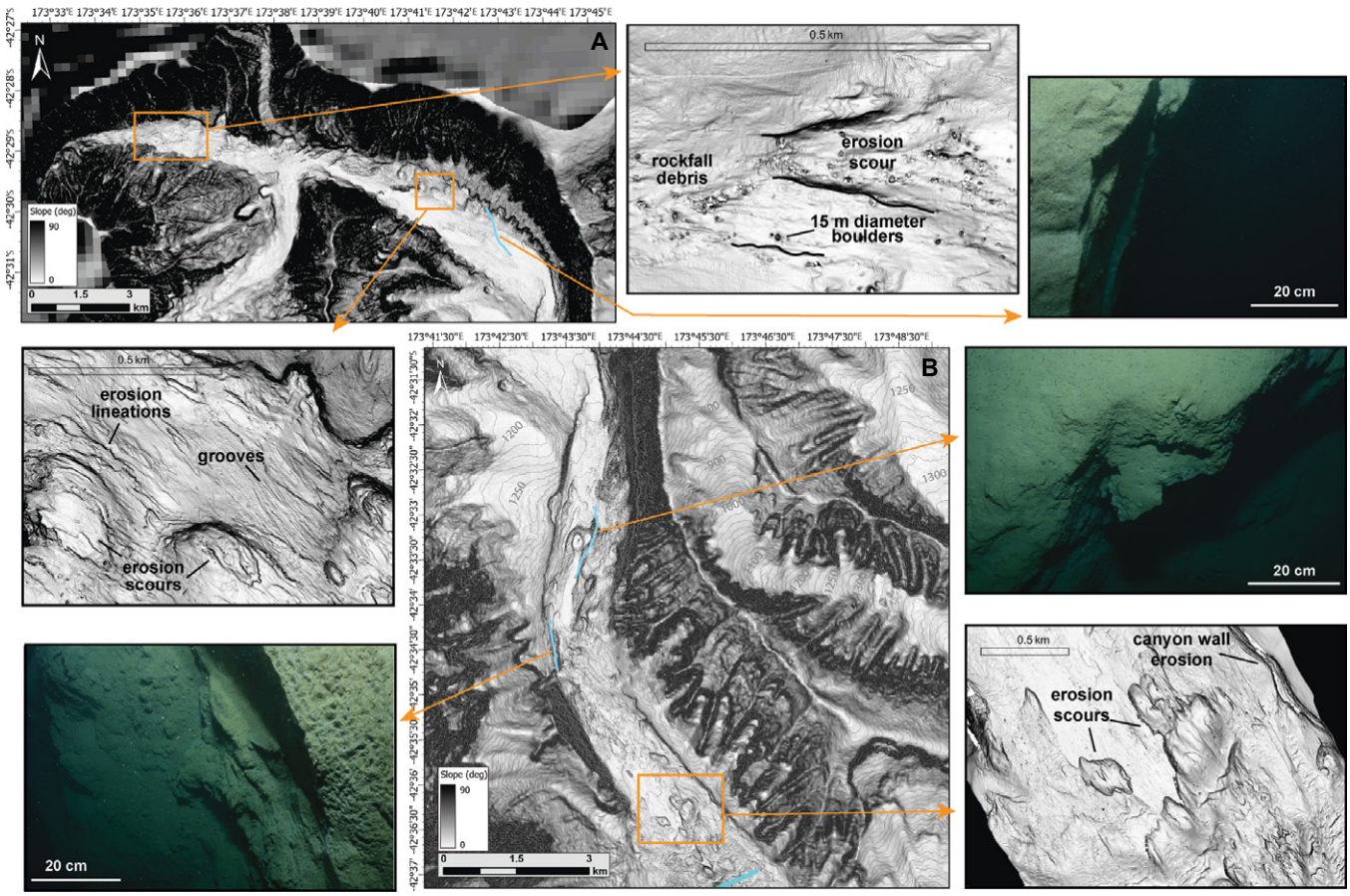

Figure 2. Slope gradient maps of the upper Kaikōura Canyon (Aotearoa–New Zealand). Zoom-in areas (orange boxes) show detail of erosional features. Deep-towed imaging system (DTIS) seafloor imagery (light-blue lines) show evidence of bedrock erosion.

DISCUSSION

Bedrock Erosion in Kaikōura Canyon

During the 2016 earthquake, large amounts of coarse (gravel to boulder) sediment previously accumulated in the Kaikōura Canyon rim was mobilized downcanyon (Fig. 4A). The high availability of gravel and boulder blocks likely produced a thick and coarse-grained debris flow front, increasing the impact forces on the canyon floor (Ilstad et al., 2004; Roelofs et al., 2022). We infer that the transport of coarse debris during the flushing event is the primary mechanism for bedrock erosion in the canyon head and upper canyon, and potentially initiated the excavation of the bedrock in the canyon axis and walls (Fig. 4A).

Exposed bedrock is rarely documented in the axis of submarine canyons, which are normally obscured by unconsolidated sediments (Paull et al., 2011). In our study, the grooves and erosional scours revealed in the high-resolution bathymetry (Fig. 2; Fig. S1) provide evidence that dense debris flows remobilized and transported coarse sediment, eroding bedrock in the upper canyon. We interpret the grooves as caused by removal of semi-consolidated canyon-floor material, whereas the erosive scours suggest that the bed failed under the influence of the debris flow, a process of plucking or quarrying in which bedrock blocks erode along rock defects and fractures (Mitchell, 2014; Smith et al., 2018; Zhang et al., 2020).

Flow Transformation: Debris Flow to Turbidity Current

The Kaikōura Canyon debris flow (with dominant erosion) is interpreted to have transformed into a turbidity current (depositional regime) at mid-canyon (~1450 m water depth), where the canyon axis abruptly doubles in width (Fig. 3A). At that location, we observe the development of depositional features (gravel waves and cyclic steps) alongside erosional scours, which create knickpoint-inducing hydraulic jumps (Fig. 4B). This suggests the potential dilution of the gravity flow, inducing the transformation from the debris flow to a turbidity current (Felix and Peakall, 2006), which can be caused by incorporation of ambient water at a hydraulic jump, or at the upper surface of the flow, or by liquefaction and acceleration of the debris flow leading to increased turbulence (Felix et al., 2009).

Variations of Gravity Flow (Turbidity Current) Dynamics

Changes in the turbidity flow dynamics during a canyon flushing event will influence the deposition of the sediment. These variations in flow dynamics are commonly associated with hydraulic jumps on the base of knickpoint and changes of orientation and width of the canyon axis (i.e., turning points affect the flow velocity) (Arzola et al., 2008; Talling et al., 2015), all of which are observed in Kaikōura Canyon.

The coexistence of gravel waves and cyclic steps across the mid-canyon axis suggests changes in the dynamics of the turbidity current during the canyon flushing event (Fig. 3; Fig. S3). Cyclic steps develop immediately downstream of erosional scours, which may have acted as knickpoints during the 2016 flow, constraining the extension of the train of cyclic steps (Fig. 3A). The cyclic step wavelength gradually decreases downstream of the knickpoint; the down-canyon transitions of these features from steep lee slopes to gentle stoss slopes are interpreted to have caused hydraulic jumps in the flow (supercritical to subcritical regimes), leading to local deposition on stoss slopes (Fig. 3A; Fig. S3). Moreover, the variation in morphology of the gravel waves downcanyon (i.e., planform crest shape, height, and wavelength; Fig. 3B; Fig. S2) also suggests potential flow deceleration downcanyon and/or the transformation of flow dynamics across- and downcanyon.

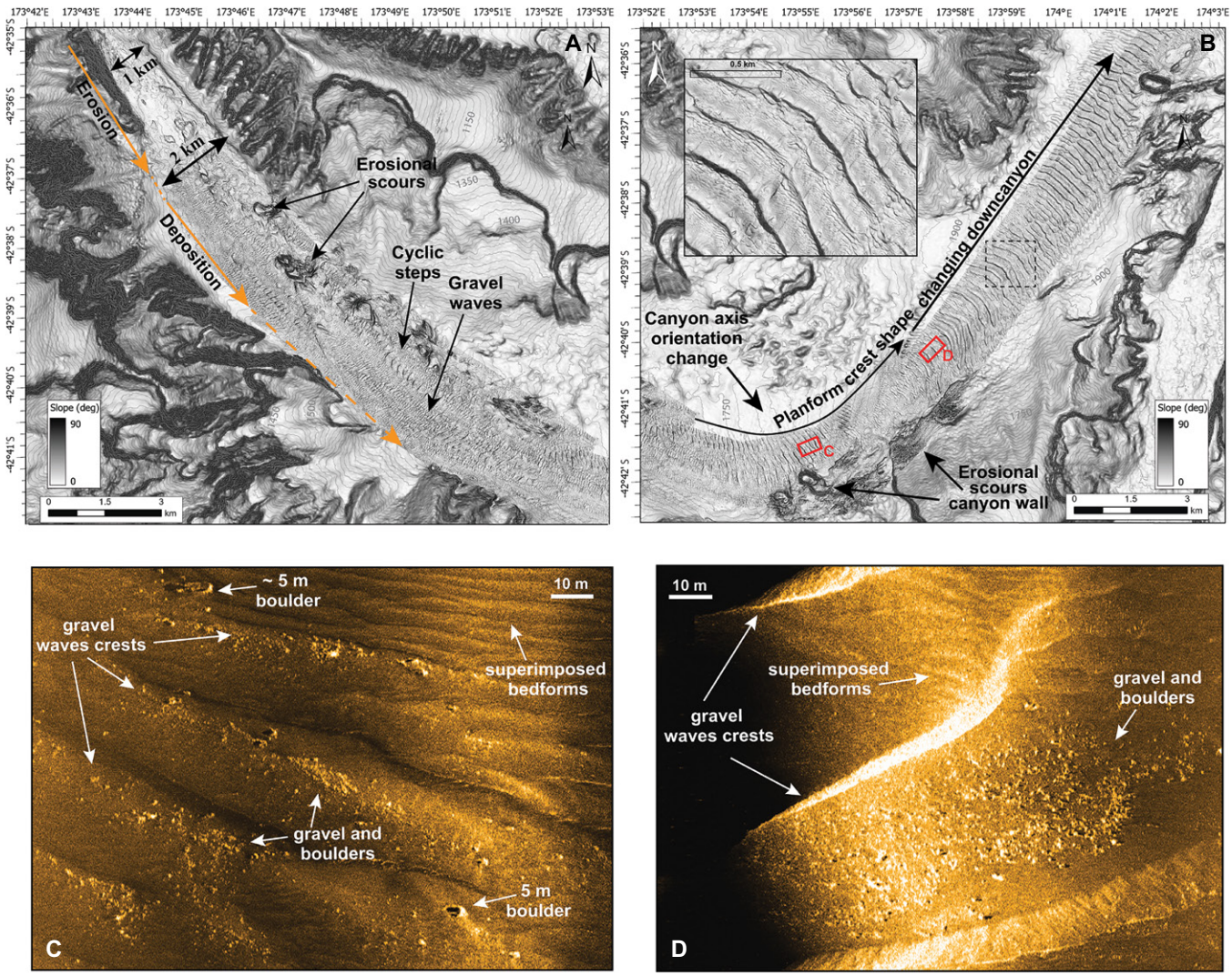

Figure 3. (A, B) Slope gradient maps of Kaikōura Canyon (Aotearoa–New Zealand). (A) Mid-canyon, showing the transition from an erosional to depositional regime (orange lines) with the co-existence of erosive scours, gravel waves, and cyclic steps. (B) Lower canyon with detail of the change of gravel-waves planform crest shape downcanyon. Zoom-in inset (dashed-line box) shows superimposed bedforms on top of the gravel waves. (C, D) Side-scan sonar images (locations shown by red rectangles in panel B) revealing large boulders over the gravel waves (side-scan sonar images show intensity of the return signal; dark colors indicate low intensity corresponding to finer sediment).

Farther downcanyon, the presence of very large boulders on top of the large gravel waves at the lower canyon (Fig. 3) are interpreted as being deposited during the transformation to subcritical flow. Settling of such large boulders leaves the remaining flow diluted, and may cause it to accelerate, leading to an increase of current turbulence (Felix and Peakall, 2006). This is supported by sediment samples collected along the mid- and lower canyon four days after the Kaikōura earthquake, which revealed highly fluidized and normally graded turbidites (Mountjoy et al., 2018). However, it is worth noting the numerous landslide scars, identified at the upper part of the canyon walls along the mid- and lower canyon (from ~1100 m down to ~1780 m water depth; Figs. 1, 2B, and 3A). These could have been triggered during the 2016 earthquake, increasing the sediment load feeding the turbidity current downcanyon.

We suggest the turbidity current was internally stratified (i.e., vertical gravity segregation of particles) based on the observations from the lower part of Kaikōura Canyon: (1) the presence of small-scale superimposed dunes over the large gravel waves, interpreted to arise from deposition of particles from the finer upper layer of a turbidity current (Fig. 3B); and (2) the erosive lineations observed on the outer bend (where the axis orientation changes from northwest-southeast to northeast-southwest; Figs. 3B–3D), reaching heights of ~150–200 m above the canyon floor in the canyon wall (Fig. 3B), which are indicative of an eroding dense basal layer near the flow front. This is consistent with the calculated minimum flow height of ~180 m at the lower part of Kaikōura Canyon (Howarth et al., 2021; Mountjoy et al., 2018).

CONCLUSIONS

Our observations provide new insights into gravity flow dynamics during canyon flushing events, specifically (1) gravity flow transformation (debris flow to turbidity current) occurring between the constricted upper canyon and the more open mid-canyon; and (2) dynamic variations within the turbidity current across- and downcanyon, influenced by canyon morphology (i.e., abrupt changes in canyon axis width and orientation).

We suggest that, during submarine canyon flushing events, high-energy, high-density, coarse-grained debris flows erode the upper canyon, exposing the bedrock. At mid-canyon, the presence of grooves and erosive scours

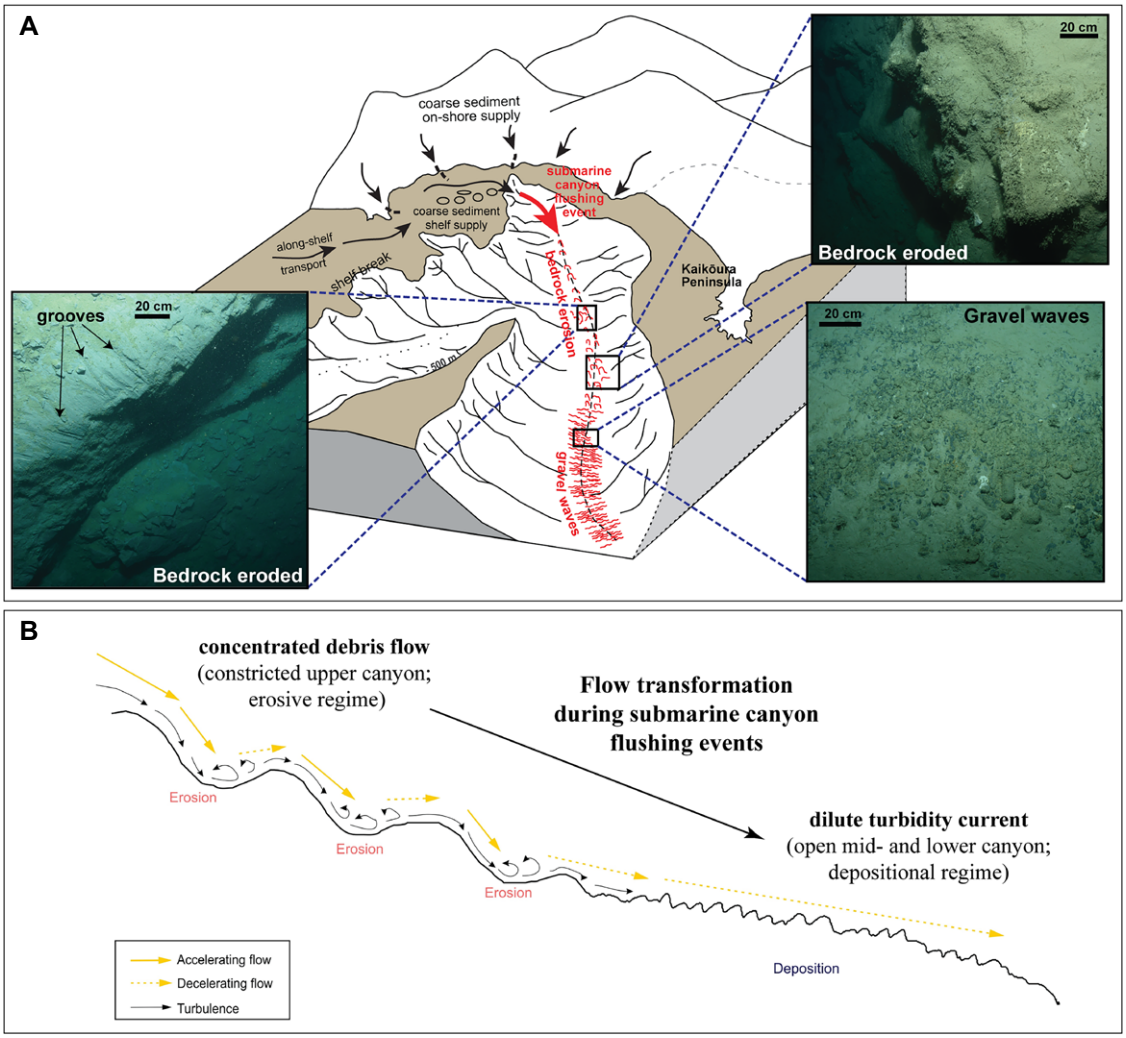

Figure 4. (A) Schematic diagram of the 2016 Kaikōura Canyon (Aotearoa–New Zealand) flushing event. Deep-towed imaging system (DTIS) seafloor imagery shows erosional and depositional features. (B) Conceptual model of the transformation of the debris flow into a turbidity current downcanyon.

are jointly observed with depositional coarse-grained bedforms, suggesting a transformation of flow, from concentrated debris flow to dilute turbidity current. From mid-canyon, the canyon floor transitions to being dominated by gravel waves that vary in size, planform crest shape, and orientation. These variations record changes in the turbidity current dynamics, with variations of threshold shear stress and flow acceleration both across- and downcanyon.

Our study provides detailed geomorphological observations that have enabled us to reconstruct transformations of flow dynamics during the 2016 submarine canyon flushing event in Kaikōura Canyon. This research will enhance our understanding of gravity flow dynamics and erosion in bedrock submarine canyons worldwide.

ACKNOWLEDGMENTS

We appreciate the ongoing support of Te Rūnanga ō Kaikōura for scientific research in Kaikōura Canyon. We acknowledge the science and ship crews of TAN2011 (New Zealand National Institute of Water and Atmospheric Research [NIWA] cruise); funding from Eurofleets, the NIWA Strategic Science Investment Fund, and University of Auckland Faculty Research Development Fund grant ESSIBE4798128; and vessel time from the New Zealand Ministry of Business, Innovation & Employment (MBIE) Tangaroa Reference Group. We thank the University of Gothenburg (Sweden) staff for the guidance and technical support on operating Kongsberg Maritime's HUGIN AUV. We thank the editor Kathleen Benison, reviewers Silvia Ceramicola and Jake Covault, and an anonymous reviewer, for helping us improve earlier versions of this manuscript.

REFERENCES CITED

Amy, L.A., and Talling, P.J., 2006, Anatomy of turbidites and linked debrites based on long distance (120 × 30 km) bed correlation, Marnoso Arenacea Formation, Northern Apennines, Italy: Sedimentology, v. 53, p. 161–212, https://doi.org/10.1111/j.1365-3091.2005.00756.x.

Arzola, R.G., Wynn, R.B., Lastras, G., Masson, D.G., and Weaver, P.P., 2008, Sedimentary features and processes in the Nazaré and Setúbal submarine canyons, west Iberian margin: Marine Geology, v. 250, p. 64–88, https://doi.org/10.1016/j.margeo.2007.12.006.

Bernhardt, A., and Schwanghart, W., 2021, Where and why do submarine canyons remain connected to the shore during sea-level rise? Insights from global topographic analysis and Bayesian regression: Geophysical Research Letters, v. 48, https://doi.org/10.1029/2020GL092234.

Cartigny, M.J.B., Postma, G., van den Berg, J.H., and Mastbergen, D.R., 2011, A comparative study of sediment waves and cyclic steps based on geometries, internal structures and numerical modeling: Marine Geology, v. 280, p. 40–56, https://doi.org/10.1016/j.margeo.2010.11.006.

Covault, J.A., and Graham, S.A., 2010, Submarine fans at all sea-level stands: Tectono-morphologic and climatic controls on terrigenous sediment delivery to the deep sea: Geology, v. 38, p. 939–942, https://doi.org/10.1130/G31081.1.

Felix, M., and Peakall, J., 2006, Transformation of debris flows into turbidity currents: Mechanisms inferred from laboratory experiments: Sedimentology, v. 53, p. 107–123, https://doi.org/10.1111/j.1365-3091.2005.00757.x.

Felix, M., Leszczyński, S., Ślączka, A., Uchman, A., Amy, L., and Peakall, J., 2009, Field expressions of the transformation of debris flows into turbidity currents, with examples from the Polish Carpathians and the French Maritime Alps: Marine and Petroleum Geology, v. 26, p. 2011–2020, https://doi.org/10.1016/j.marpetgeo.2009.02.014.

Fisher, R.V., 1983, Flow transformations in sediment gravity flows: Geology, v. 11, p. 273–274, https://doi.org/10.1130/0091-7613(1983)11<273:FTISGF>2.0.CO;2.

Gibbs, M., et al., 2020, Novel application of a compound-specific stable isotope (CSSI) tracking technique demonstrates connectivity between terrestrial and deep-sea ecosystems via subma-

rine canyons: Frontiers in Marine Science, v. 7, https://doi.org/10.3389/fmars.2020.00608.
Harris, P.T., and Whiteway, T., 2011, Global distribution of large submarine canyons: Geomorphic differences between active and passive continental margins: Marine Geology, v. 285, p. 69–86, https://doi.org/10.1016/j.margeo.2011.05.008.
Haughton, P., Davis, C., McCaffrey, W., and Barker, S., 2009, Hybrid sediment gravity flow deposits—Classification, origin and significance: Marine and Petroleum Geology, v. 26, p. 1900–1918, https://doi.org/10.1016/j.marpetgeo.2009.02.012.
Haughton, P.D., Barker, S.P., and McCaffrey, W.D., 2003, 'Linked' debrites in sand-rich turbidite systems–origin and significance: Sedimentology, v. 50, p. 459–482, https://doi.org/10.1046/j.1365-3091.2003.00560.x.
Howarth, J.D., et al., 2021, Calibrating the marine turbidite palaeoseismometer using the 2016 Kaikōura earthquake: Nature Geoscience, v. 14, p. 161–167, https://doi.org/10.1038/s41561-021-00692-6.
Ilstad, T., Elverhøi, A., Issler, D., and Marr, J.G., 2004, Subaqueous debris flow behaviour and its dependence on the sand/clay ratio: A laboratory study using particle tracking: Marine Geology, v. 213, p. 415–438, https://doi.org/10.1016/j.margeo.2004.10.017.
Kostic, S., 2011, Modeling of submarine cyclic steps: Controls on their formation, migration, and architecture: Geosphere, v. 7, p. 294–304, https://doi.org/10.1130/GES00601.1.
Kuenen, P.H., and Hough, J.L., 1951, Properties of turbidity currents of high density, *in* Hough, J.L., ed., Turbidity Currents and the Transportation of Coarse Sediments to Deep Water: Tulsa, Oklahoma, Society for Sedimentary Geology (SEPM) Special Publication Number 2, p. 14–33, https://doi.org/10.2110/pec.51.02.0014.
Lewis, K.B., and Barnes, P.M., 1999, Kaikoura Canyon, New Zealand: Active conduit from nearshore sediment zones to trench-axis channel: Marine Geology, v. 162, p. 39–69, https://doi.org/10.1016/S0025-3227(99)00075-4.
Micallef, A., Ribó, M., Canals, M., Puig, P., Lastras, G., and Tubau, X., 2014, Space-for-time substitution and the evolution of a submarine canyon–channel system in a passive progradational margin: Geomorphology, v. 221, p. 34–50, https://doi.org/10.1016/j.geomorph.2014.06.008.
Middleton, G.V., and Hampton, M.A., 1973, Sediment gravity flows: Mechanics of flow and deposition: Turbidites and Deep Water Sedimentation: Society for Sedimentary Geology (SEPM) Pacific Section Short Course Notes, Part 1, p. 1–38.
Mitchell, N.C., 2005, Interpreting long-profiles of canyons in the USA Atlantic continental slope: Marine Geology, v. 214, p. 75–99, https://doi.org/10.1016/j.margeo.2004.09.005.
Mitchell, N.C., 2014, Bedrock erosion by sedimentary flows in submarine canyons: Geosphere, v. 10, p. 892–904, https://doi.org/10.1130/GES01008.1.
Mitchell, J.S., Mackay, K.A., Neil, H.L., Mackay, E.J., Pallentin, A., and Notman, P., 2012, Undersea New Zealand, 1:5,000,000, NIWA Chart, Miscellaneous Series no. 92.
Mountjoy, J.J., et al., 2018, Earthquakes drive large-scale submarine canyon development and sediment supply to deep-ocean basins: Science Advances, v. 4, https://doi.org/10.1126/sciadv.aar3748.
Nokes, C.R., Bostock, H.C., Strachan, L.J., and Hadfield, M.G., 2021, Hydrodynamics and sediment transport on the North Canterbury Shelf, New Zealand: New Zealand Journal of Marine and Freshwater Research, v. 55, p. 112–131, https://doi.org/10.1080/00288330.2019.1699584.
Normark, W.R., and Carlson, P.R., 2003, Giant submarine canyons: Is size any clue to their importance in the rock record? *in* Chan, M.A., and Archer, A.W., eds., Extreme Depositional Environments: Mega End Members in Geologic Time: Geological Society of America Special Paper 370, p. 175–190, https://doi.org/10.1130/0-8137-2370-1.175.
Parker, G., 1996, Some speculations on the relation between channel morphology and channel-scale flow structures, *in* Ashworth, P.J., et al., eds., Coherent Flow Structures in Open Channels: Chichester, Wiley, p. 423–458.
Paull, C.K., Caress, D.W., Ussler, W., III, Lundsten, E., and Meiner-Johnson, M., 2011, High-resolution bathymetry of the axial channels within Monterey and Soquel submarine canyons, offshore central California: Geosphere, v. 7, p. 1077–1101, https://doi.org/10.1130/GES00636.1.
Ribó, M., Puig, P., Muñoz, A., Lo Iacono, C., Masqué, P., Palanques, A., Acosta, J., Guillén, J., and Gómez Ballesteros, M., 2016, Morphobathymetric analysis of the large fine-grained sediment waves over the Gulf of Valencia continental slope (NW Mediterranean): Geomorphology, v. 253, p. 22–37, https://doi.org/10.1016/j.geomorph.2015.09.027.
Roelofs, L., Colucci, P., and de Haas, T., 2022, How debris-flow composition affects bed erosion quantity and mechanisms: An experimental assessment: Earth Surface Processes and Landforms, v. 47, p. 2151–2169, https://doi.org/10.1002/esp.5369.
Smith, M.E., Werner, S.H., Buscombe, D., Finnegan, N.J., Sumner, E.J., and Mueller, E.R., 2018, Seeking the shore: Evidence for active submarine canyon head incision due to coarse sediment supply and focusing of wave energy: Geophysical Research Letters, v. 45, p. 12,403–12,413, https://doi.org/10.1029/2018GL080396.
Stow, D., and Smillie, Z., 2020, Distinguishing between deep-water sediment facies: Turbidites, contourites and hemipelagites: Geosciences, v. 10, 68, https://doi.org/10.3390/geosciences10020068.
Talling, P., Amy, L., Wynn, R., Peakall, J., and Robinson, M., 2004, Beds comprising debrite sandwiched within co-genetic turbidite: Origin and widespread occurrence in distal depositional environments: Sedimentology, v. 51, p. 163–194, https://doi.org/10.1111/j.1365-3091.2004.00617.x.
Talling, P.J., 2014, On the triggers, resulting flow types and frequencies of subaqueous sediment density flows in different settings: Marine Geology, v. 352, p. 155–182, https://doi.org/10.1016/j.margeo.2014.02.006.
Talling, P.J., Allin, J., Armitage, D.A., Arnott, R.W., Cartigny, M.J., Clare, M.A., Felletti, F., Covault, J.A., Girardclos, S., and Hansen, E., 2015, Key future directions for research on turbidity currents and their deposits: Journal of Sedimentary Research, v. 85, p. 153–169, https://doi.org/10.2110/jsr.2015.03.
Wang, J., La Croix, A.D., Wang, H., Pang, X., and Liu, B., 2024, Flume experiments of gravity flows: Transformation from sandy debris flows to turbidity currents with clay matrix separation: Sedimentary Geology, v. 461, https://doi.org/10.1016/j.sedgeo.2023.106576.
Zhang, L., Li, T., Wang, G., Kwang, J.S., Nittrouer, J.A., Fu, X., and Parker, G., 2020, How canyons evolve by incision into bedrock: Rainbow Canyon, Death Valley National Park, United States: Proceedings of the National Academy of Sciences of the United States of America, v. 117, p. 14730–14737, https://doi.org/10.1073/pnas.1911040117.

Printed in the USA